Research Square

Preprints are preliminary reports that have not undergone peer review.
They should not be considered conclusive, used to inform clinical practice,
or referenced by the media as validated information.

Quantitative 18 F-Fluciclovine PET for Differentiating Brain Tumors from Non-Tumor Lesions in Patients with Suspected Malignant Glioma

Ryu Saito
University of Yamanashi
Mitsuto Hanihara
mhanihara@yamanashi.ac.jp
University of Yamanashi
Hirofumi Kazama
University of Yamanashi
Hideyuki Yoshioka
University of Yamanashi

Research Article

Keywords: 18F-fluciclovine, glioma, positron emission tomography, non-tumor lesion, radiation necrosis, demyelinating disease

Posted Date: November 20th, 2026

DOI: https://doi.org/10.21203/rs.3.rs-11550364/v1

License: This work is licensed under a Creative Commons Attribution 4.0 International License.
Read Full License

Additional Declarations: No competing interests reported.

Quantitative ^{18}F-Fluciclovine PET for Differentiating Brain Tumors from Non-Tumor Lesions in Patients with Suspected Malignant Glioma

Ryu Saito, Mitsuto Hanihara, Hirofumi Kazama, Hideyuki Yoshioka

Department of Neurosurgery, University of Yamanashi, 1110 Shimokato, Chuo City, Yamanashi 409-3898, Japan

Corresponding author
Mitsuto Hanihara, MD, PhD
Department of Neurosurgery, University of Yamanashi
1110 Shimokato, Chuo, Yamanashi 409-3898, Japan
E-mail: mhanihara@yamanashi.ac.jp

Abstract

Purpose: Contrast-enhancing lesions suspected to be malignant glioma often demonstrate non-specific magnetic resonance imaging (MRI) findings. This study aimed to characterize ^{18}F-fluciclovine uptake and the diagnostic performance of quantitative positron emission tomography (PET) parameters among gliomas, non-glioma tumors, and non-tumors.

Methods: This retrospective analysis included 26 patients who underwent preoperative ^{18}F-fluciclovine PET for contrast-enhancing lesions suspected to be malignant glioma and subsequently underwent pathological evaluation. Maximum and peak standardized uptake values (SUVmax and SUVpeak) and their corresponding tumor-to-background ratios (T/B and Tpeak/B ratios) were compared. Diagnostic performance was explored via receiver operating characteristic analysis.

Results: The cohort was comprised of 13, 9, and 4 patients with gliomas, non-glioma tumors, and non-tumor lesions, respectively. SUVmax, SUVpeak, T/B ratio, and Tpeak/B ratio significantly differed among the three groups, but background white matter uptake showed no significant difference. On post hoc analysis all four parameters were significantly higher in both tumor groups versus the non-tumor group, with no significant differences between the two tumor groups. Exploratory ROC analysis showed AUCs of 0.981 for both SUVmax and SUVpeak and 0.962 for both T/B and Tpeak/B ratios for differentiating glioma from non-tumor lesions.

Conclusion: Among contrast-enhancing lesions suspected to be malignant glioma, quantitative ^{18}F-fluciclovine PET parameters, particularly SUVmax, SUVpeak, and background-corrected uptake ratios, may help distinguish tumors from non-tumor lesions. However, because non-glioma tumors also showed high uptake, ^{18}F-fluciclovine PET cannot be solely used to distinguish gliomas from other tumors. These exploratory findings require validation in larger independent cohorts.

Keywords

^{18}F-fluciclovine; glioma; positron emission tomography; non-tumor lesion; radiation necrosis; demyelinating disease

Introduction

In clinical neuro-oncology, contrast-enhancing lesions suspected to be malignant glioma often pose a diagnostic challenge. Conventional magnetic resonance imaging (MRI) findings are often non-specific as well. For appropriate clinical management, it is crucial to distinguish gliomas from other tumors and non-tumor lesions, such as demyelinating disease and radiation necrosis. Although making an early tissue diagnosis is important when suspecting tumors, both biopsy and resection are invasive procedures. Therefore, the surgical indications, operative strategy, and sampling targets must be carefully considered.

Amino acid positron emission tomography (PET) has attracted increasing attention as a molecular imaging technique that complements contrast-enhanced MRI by providing information on amino acid transporter activity and tumor metabolism [1]. ^{18}F-fluciclovine (anti-1-amino-3-^{18}F-fluorocyclobutane-1-carboxylic acid; FACBC) is a synthetic amino acid tracer which is used in Japan for tumor visualization in patients with suspected malignant glioma, particularly as an adjunct for planning the extent of surgical resection [2]. ^{18}F-fluciclovine uptake is mediated, at least in part, by neutral amino acid transporters, including alanine-serine-cysteine transporter 2 (ASCT2) and L-type amino acid transporter (LAT) family transporters [3, 4]. Additionally, in contrast-enhancing lesions, radiotracer accumulation may also be affected by local factors such as blood-brain barrier (BBB) disruption and vascular permeability [4]. Thus, tracer uptake likely reflects both tumor-cell transport activity and the lesional microenvironment.

Previous studies have demonstrated the clinical utility of ^{18}F-fluciclovine PET in glioma detection, tumor delineation, and recurrent brain tumor assessment [2, 5-8]. However, ^{18}F-fluciclovine uptake is not specific to gliomas. Non-tumor lesions may also demonstrate accumulation due to inflammation, tissue repair, altered perfusion, or BBB disruption, and various non-glioma tumors can similarly exhibit substantial uptake. Recent reports have described fluciclovine uptake in low-grade and benign lesions and a tumefactive demyelinating lesion [9, 10]. Despite its increasing clinical use in patients with suspected malignant glioma, the utility of ^{18}F-fluciclovine PET has not been systematically evaluated across the spectrum of contrast-enhancing lesions in this setting; its ability to distinguish gliomas from other tumors and non-tumor lesions remains unclear.

This retrospective analysis evaluated patients who underwent preoperative ^{18}F-fluciclovine PET for contrast-enhancing lesions clinically suspected to be malignant glioma and who subsequently received a pathological diagnosis after resection or biopsy. Quantitative PET parameters were calculated from regions of interest placed within the enhancing lesion and compared among three final diagnostic groups: glioma, non-glioma tumor, and non-tumor. This study aimed to characterize ^{18}F-fluciclovine uptake among the three diagnostic groups and to explore the diagnostic performance of quantitative PET parameters for distinguishing gliomas from non-glioma tumors and non-tumor lesions.

Materials and Methods

Study Design and Ethics

This retrospective observational study was conducted at a single institution. The study was conducted in accordance with the Declaration of Helsinki and relevant ethical guidelines for clinical research [11]. The study protocol was approved by the University of Yamanashi Ethics Committee (approval no. 2845). The requirement for individual informed consent was waived by the ethics committee, and an opt-out procedure was implemented to allow patients to decline the use of their clinical data for research. All patient data were de-identified before analysis.

Patients

This study retrospectively included 26 consecutive patients who underwent preoperative ^{18}F-fluciclovine PET between July 2024 and June 2026 for lesions suspected to be malignant glioma on contrast-enhanced MRI. The suspicion of malignant glioma was made by the treating neurosurgical team based on preoperative contrast-enhanced MRI findings. Surgical resection or biopsy was considered necessary in these patients. At our institution, ^{18}F-fluciclovine PET was available for only one patient once a week. Thus, PET was only performed when scheduling was feasible before surgery, whereas patients requiring urgent surgical intervention proceeded to surgery without PET. All 26 patients included in this study subsequently underwent surgical resection or biopsy, and a histopathological diagnosis was obtained in all cases.

Tissue sampling was performed from lesions identified on contrast-enhanced MRI with reference to the PET findings. The final diagnosis was established via histopathological examination of the surgical specimens. Tumors were classified according to the 2021 World Health Organization Classification of Tumors of the Central Nervous System [12]. Patients were assigned to three groups based on the final pathological diagnosis: glioma, non-glioma tumor, or non-tumor. The non-glioma tumor group included diffuse large B-cell lymphoma (DLBCL) and meningiomas, whereas the non-tumor group included radiation necrosis and demyelinating disease.

PET and MRI Acquisition

All patients underwent preoperative ^{18}F-fluciclovine PET and MRI. PET examinations were performed in accordance with relevant guidelines and institutional protocols [2]. A fixed dose of 185 MBq of ^{18}F-fluciclovine was administered intravenously, followed by brain PET acquisition 15–20 minutes after injection. PET images were acquired using a Biograph Horizon-4R scanner (Siemens Healthineers, Erlangen, Germany) with an acquisition time of 10 minutes. The reconstruction parameters were as follows: 8 iterations, 10 subsets, image size 256, zoom factor 2.0, Gaussian filter, and full width at half maximum of 4.0 mm. MRI was performed using either a 1.5-T or 3-T scanner (Optima 450 or Discovery 750; GE Healthcare, WI, USA). The imaging protocol included T1-weighted imaging (T1WI; slice thickness < 5 mm), fluid-attenuated inversion recovery (FLAIR) imaging (slice thickness < 5 mm), and contrast-enhanced T1WI (slice thickness < 1.2 mm). Contrast-enhanced T1WI was acquired via three-dimensional T1-weighted gradient-echo sequence after intravenous administration of a standard dose of gadolinium-based contrast agent (0.1 mmol/kg).

Image Analysis

Co-registration of contrast-enhanced T1WI and PET images was performed using SYNAPSE VINCENT (Fujifilm, Tokyo, Japan; version 7.0.0003). Automatic rigid registration was first performed and manually corrected when necessary. Regions of interest (ROIs) were manually delineated on contrast-enhanced T1WI with reference to the co-registered PET images to encompass the contrast-enhancing component, while avoiding physiological uptake and obvious imaging artifacts where possible. If multiple lesions were present, then the lesion with the largest maximum diameter on contrast-enhanced T1WI was selected for analysis. SUVmax was defined as the maximum standardized uptake value (SUV) within the ROI. SUVpeak was defined as the mean SUV within a fixed 1.0 mL spherical volume of interest (VOI) centered on the area of highest uptake within the lesion. For background measurement, a spherical VOI (diameter: 10-mm) was placed in the contralateral normal-appearing white matter, centered on the same axial level as the center of the lesion. The mean SUV within this background VOI was defined as SUVmean_B. Background VOIs were placed to avoid tumor, edema, hemorrhage, infarction, and imaging artifacts. The tumor-to-background (T/B) ratio was calculated as SUVmax / SUVmean_B. The peak tumor-to-background (Tpeak/B) ratio was calculated as SUVpeak / SUVmean_B.

Pathological Evaluation

Surgical specimens were processed as formalin-fixed, paraffin-embedded tissue. Hematoxylin and eosin staining was performed. Immunohistochemistry included glial fibrillary acidic protein (GFAP), Olig2, MIB-1 (Ki-67), IDH1 R132H, p53, and ATRX in glioma cases. Tumors were diagnosed based on the 2021 WHO Classification of Tumors of the Central Nervous System [12]. Non-tumor diagnoses were established based on histopathological findings. When required for integrated diagnosis, additional molecular analyses were performed, including *IDH* sequencing, 1p/19q codeletion testing, and *TERT* promoter mutation analysis. The Ki-67 labeling index was assessed using the hotspot method.

Statistical Analysis

Statistical analyses were performed using Python (version 3.13.9) with the NumPy, pandas, SciPy, scikit-posthocs, and scikit-learn libraries. Statistical figures were generated using Matplotlib. For patient characteristics, continuous variables were summarized as mean and range. PET quantitative indices were presented as median and interquartile range. Between-group comparisons were performed using the Kruskal–Wallis test, with significant differences further subject to post hoc pairwise comparisons using Dunn's test with Holm adjustment for multiple comparisons. All tests were two-sided, with $p < 0.05$ considered statistically significant. For the exploratory evaluation of diagnostic performance, receiver operating characteristic (ROC) curve analyses were performed to differentiate glioma from non-tumor lesions. Because of the limited sample sizes of the diagnostic subgroups, ROC analysis was not performed for other pairwise comparisons. The area under the ROC curve (AUC) was calculated, with the optimal cutoff value determined using the Youden index and 95% confidence intervals (CIs) estimated using 100,000 stratified bootstrap resamples with replacement within each diagnostic group. The 2.5th and 97.5th percentiles of the bootstrap AUC distribution were used to construct the 95% CIs.

Results

Patient Characteristics

The analysis included 26 patients (Table 1), consisting of 14 males and 12 females with a mean age of 68.0 years (range, 40–87 years). Regarding surgical procedures, 13 patients each underwent resection and biopsy.

Table 1 Patient characteristics and final diagnoses

Case	Age (years)	Sex	Final diagnosis	Lesion location	Surgical procedure	Diagnostic group
1	68	F	Glioblastoma, IDH-wildtype, CNS WHO grade 4	Left thalamus	Resection	Glioma
2	74	F	Glioblastoma, IDH-wildtype, CNS WHO grade 4	Left frontal	Resection	Glioma
3	57	M	Glioblastoma, IDH-wildtype, CNS WHO grade 4	Right frontal	Resection	Glioma
4	46	M	Glioblastoma, IDH-wildtype, CNS WHO grade 4	Right parietal	Resection	Glioma
5	58	F	Glioblastoma, IDH-wildtype, CNS WHO grade 4	Left parietal	Resection	Glioma
6	71	F	Glioblastoma, IDH-wildtype, CNS WHO grade 4	Left occipital	Resection	Glioma
7	81	M	Glioblastoma, IDH-wildtype, CNS WHO grade 4	Bilateral frontal	Biopsy	Glioma
8	62	M	Glioblastoma, IDH-wildtype, CNS WHO grade 4	Bilateral parietal	Biopsy	Glioma
9	71	M	Glioblastoma, IDH-wildtype, CNS WHO grade 4	Right frontal	Biopsy	Glioma
10	83	F	Glioblastoma, IDH-wildtype, CNS WHO grade 4	Right frontoparietal	Biopsy	Glioma
11	84	F	Glioblastoma, IDH-wildtype, CNS WHO grade 4	Right thalamus	Biopsy	Glioma
12	44	F	Astrocytoma, IDH-mutant, CNS WHO grade 4	Left parietal	Resection	Glioma
13	57	M	Oligodendroglioma, IDH-mutant and 1p/19q-codeleted, CNS WHO grade 3	Right temporal	Resection	Glioma
14	77	F	Diffuse large B-cell lymphoma	Right frontal	Resection	Non-glioma tumor
15	64	M	Diffuse large B-cell lymphoma	Left temporal	Resection	Non-glioma tumor

Case	Age (years)	Sex	Final diagnosis	Lesion location	Surgical procedure	Diagnostic group
16	74	F	Diffuse large B-cell lymphoma	Right frontal	Biopsy	Non-glioma tumor
17	73	M	Diffuse large B-cell lymphoma	Left temporal	Biopsy	Non-glioma tumor
18	82	M	Diffuse large B-cell lymphoma	Bilateral frontal	Biopsy	Non-glioma tumor
19	66	M	Diffuse large B-cell lymphoma	Left frontal	Biopsy	Non-glioma tumor
20	72	M	Diffuse large B-cell lymphoma	Right thalamus	Biopsy	Non-glioma tumor
21	87	F	Atypical meningioma	Right temporoparietal	Resection	Non-glioma tumor
22	69	F	Meningothelial meningioma	Right frontal	Resection	Non-glioma tumor
23	71	M	Demyelinating disease	Bilateral parietal	Biopsy	Non-tumor
24	67	F	Demyelinating disease	Right frontal	Biopsy	Non-tumor
25	69	M	Demyelinating disease	Right frontal	Biopsy	Non-tumor
26	40	M	Radiation necrosis	Left parietal	Resection	Non-tumor

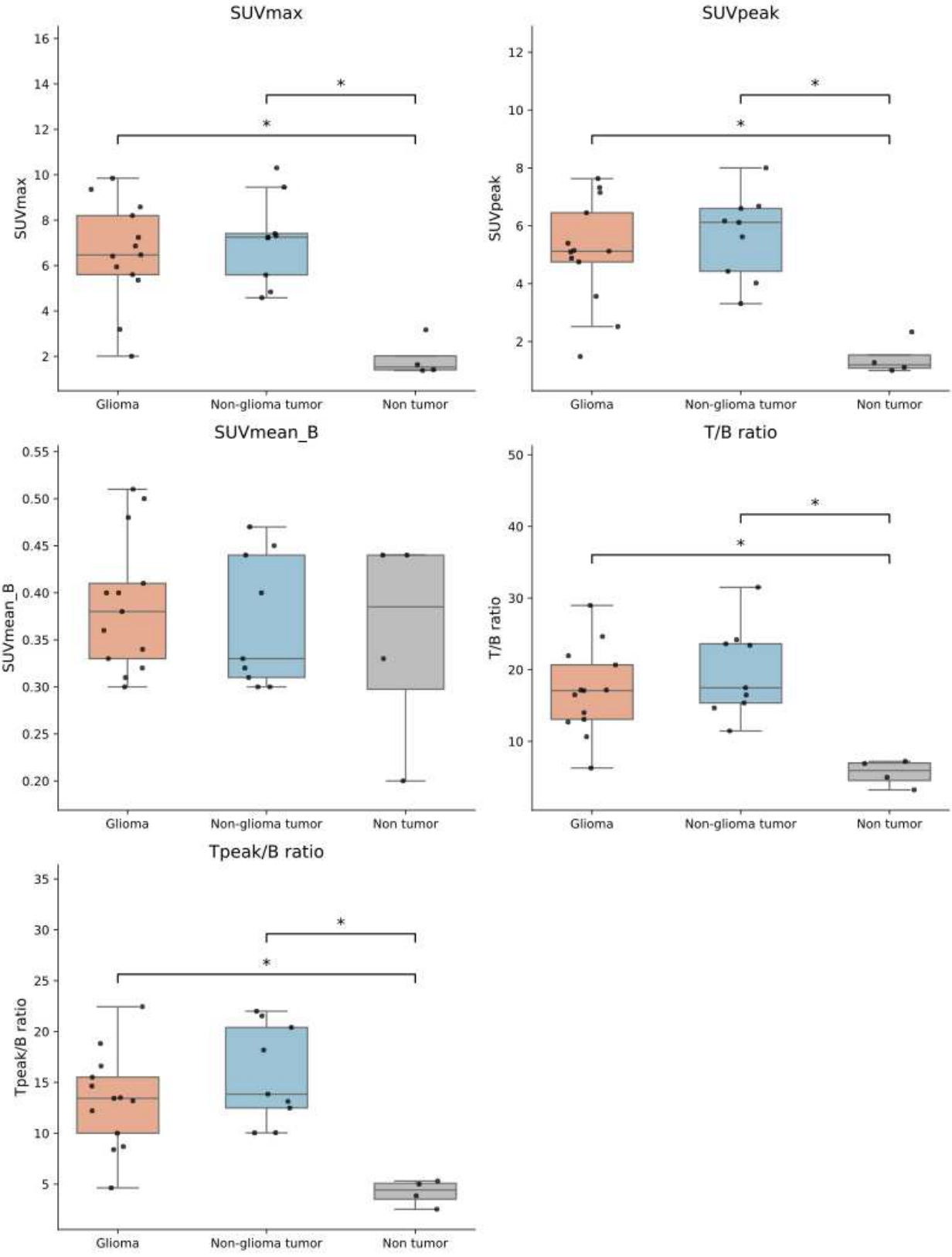
Abbreviations: CNS = central nervous system; IDH = isocitrate dehydrogenase; WHO = World Health Organization.

Diagnostic Groups

The glioma group included 13 patients with the following diagnoses: glioblastoma (n = 11); IDH-mutant astrocytoma, CNS WHO grade 4 (n = 1); and IDH-mutant and 1p/19q-codeleted oligodendroglioma, CNS WHO grade 3 (n = 1). The non-glioma tumor group included 9 patients diagnosed with DLBCL (n = 7), atypical meningioma (n = 1), and meningothelial meningioma (n = 1). The non-tumor group included 4 patients diagnosed with demyelinating disease (n = 3) and radiation necrosis (n = 1).

Quantitative PET Analysis

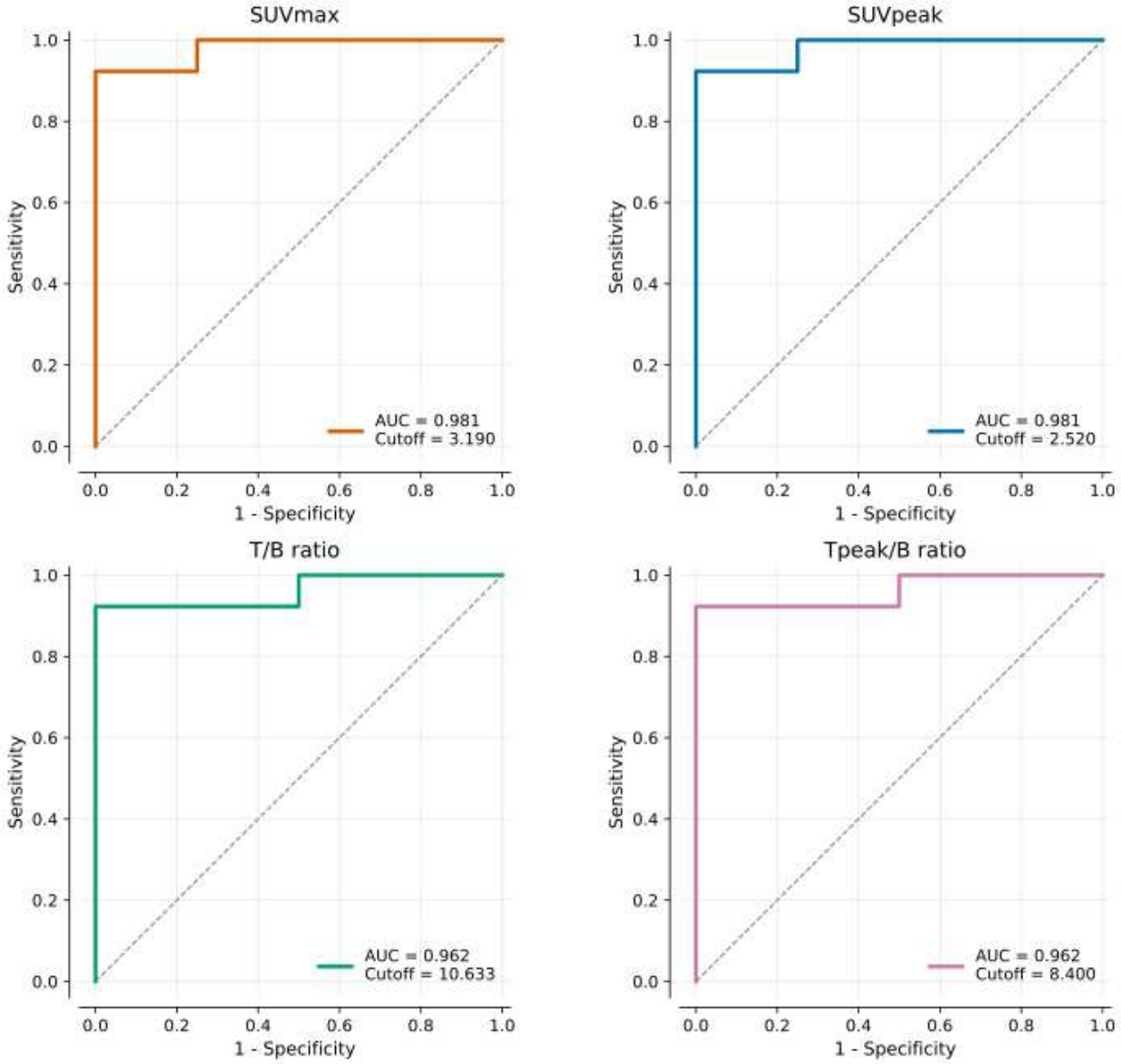
Quantitative ^{18}F-fluciclovine PET parameters are shown in Fig. 1. The glioma, non-glioma tumor, and non-tumor groups had SUVmax values (median [IQR]) of 6.47 [5.60–8.20], 7.25 [5.59–7.41], and 1.53 [1.41–2.02], respectively. The corresponding SUVpeak values were 5.12 [4.75–6.45], 6.12 [4.43–6.60], and 1.19 [1.08–1.54], respectively. The median T/B ratios were 17.08 [13.07–20.68], 17.47 [15.36–23.61], and 5.94 [4.53–6.98], while the median Tpeak/B ratios were 13.44 [10.00–15.52], 13.84 [12.49–20.40], and 4.42 [3.52–5.07], respectively. Kruskal–Wallis tests revealed significant differences among the three groups in SUVmax, SUVpeak, T/B ratio, and Tpeak/B ratio (all P = 0.008), whereas background white matter uptake had no significant difference (P = 0.752). On post hoc analyses, all four parameters were significantly higher in both the glioma and non-glioma tumor groups versus the non-tumor group, with no significant differences between the two tumor groups.


SUVmax
SUVmax
16
14
12
10
8
6
4
2
*
*
Glioma
Non-glioma tumor
Non tumor
SUVpeak
SUVpeak
12
10
8
6
4
2
*
*
Glioma
Non-glioma tumor
Non tumor
SUVmean_B
SUVmean_B
0.55
0.50
0.45
0.40
0.35
0.30
0.25
0.20
Glioma
Non-glioma tumor
Non tumor
T/B ratio
T/B ratio
50
40
30
20
10
*
*
Glioma
Non-glioma tumor
Non tumor
Tpeak/B ratio
Tpeak/B ratio
35
30
25
20
15
10
5
*
*
Glioma
Non-glioma tumor
Non tumor

172

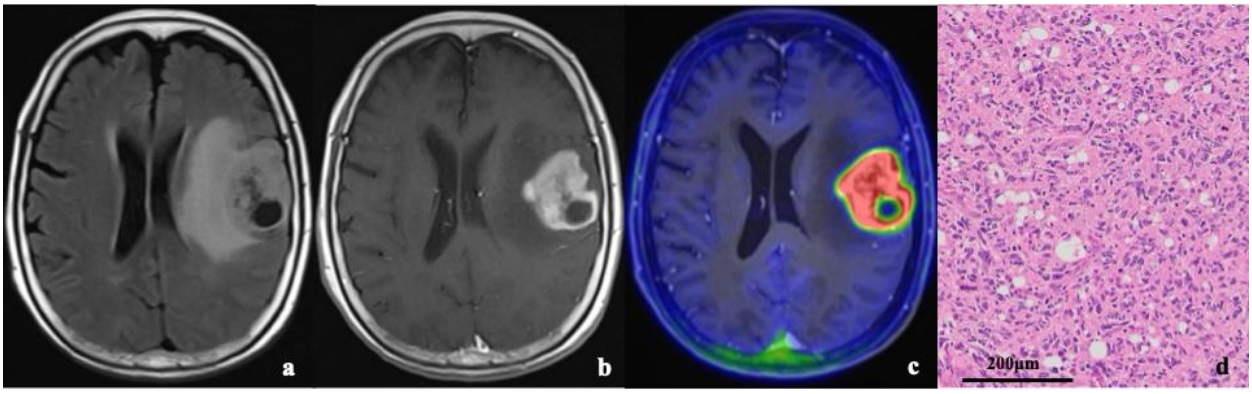
*$P < 0.05$

In the exploratory ROC analysis for differentiating glioma from non-tumor lesions, both SUVmax and SUVpeak had AUCs of 0.981 (95% CI, 0.885–1.000), while both the T/B and Tpeak/B ratios had AUCs of 0.962 (95% CI, 0.846–1.000) (Fig. 2). The Youden-derived cutoffs were 3.190, 2.520, 10.633, and 8.400, respectively. At these thresholds, each parameter had a sensitivity of 92.3% (12/13) and a specificity of 100% (4/4) in this cohort.

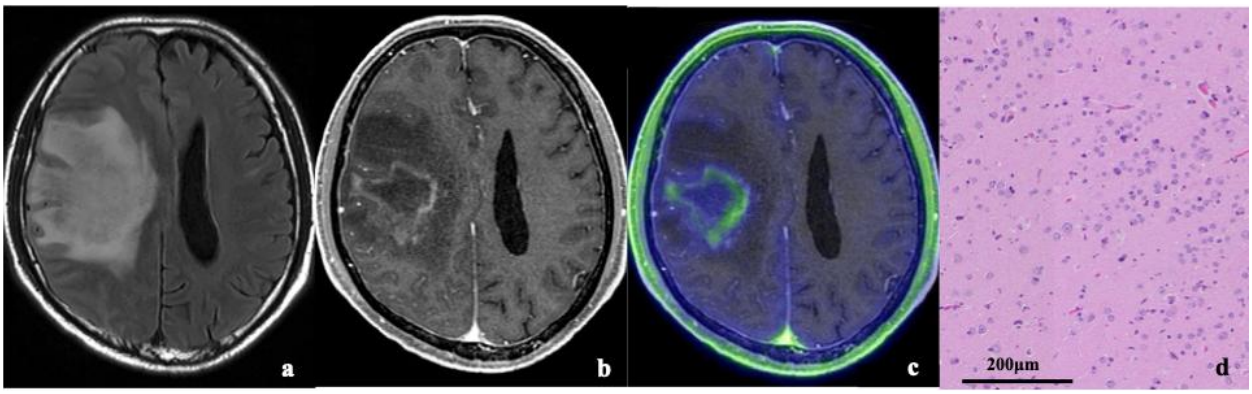


Representative Cases

Case 2 was a 74-year-old woman with a left frontal mass lesion on MRI. Contrast-enhanced T1WI showed ring enhancement, while FLAIR imaging demonstrated surrounding edema. ^{18}F-fluciclovine PET revealed high uptake corresponding to the enhancing lesion, with an SUVmax of 8.20, SUVpeak of 6.45, T/B ratio of 15.47, and Tpeak/B ratio of 12.17 (Fig. 3). The patient underwent craniotomy and tumor resection, and the pathological diagnosis was glioblastoma, IDH-wildtype.



Case 25 was a 69-year-old man with a right frontal mass lesion on MRI. Contrast-enhanced T1WI showed an irregular ring-like enhancement, while FLAIR imaging demonstrated surrounding edema. ^{18}F-fluciclovine PET demonstrated only mild uptake corresponding to the lesion, with an SUVmax of 1.38, SUVpeak of 1.00, T/B ratio of 2.60, and Tpeak/B ratio of 1.89 (Fig. 4). The patient underwent open biopsy, and the pathological diagnosis was demyelinating disease.



Discussion

This retrospective single-center study assessed the diagnostic performance of quantitative ^{18}F-fluciclovine PET metrics in patients with contrast-enhancing lesions suspected to be malignant glioma. Notably, SUVmax, SUVpeak, T/B ratio, and Tpeak/B ratio were all significantly higher in both the glioma and non-glioma tumor groups versus non-tumor lesions, whereas background white matter uptake did not differ significantly among groups. This increased uptake was observed not only in gliomas but also in non-glioma tumors. Therefore, quantitative uptake measures and tumor-to-background ratios may provide useful adjunctive information for distinguishing neoplastic from non-tumor lesions. However, because elevated uptake was not restricted to gliomas, these parameters cannot serve as specific markers for glioma.

A key novelty of this study is its focus on the differential diagnosis of contrast-enhancing lesions clinically suspected to be represent malignant glioma. Previous studies mainly examined glioma detection, tumor delineation, grading, and differentiating recurrent tumors from treatment-related changes [2, 5-8]. However, recent reports have also documented fluciclovine uptake in pilocytic astrocytoma and capillary hemangioma [9], and in a tumefactive demyelinating lesion [10], indicating that fluciclovine uptake is not specific for malignant gliomas. Nevertheless, those findings were based on individual cases and did not clarify the differences in quantitative uptake across the major pathological entities that may mimic malignant glioma on contrast-enhanced MRI. To our knowledge, no previous study has performed a cohort-level statistical comparison of quantitative ^{18}F-fluciclovine PET parameters among histopathologically confirmed gliomas, non-glioma tumors, and non-tumor lesions within the patients initially suspected to have malignant glioma. The present study builds upon previous work by systematically and quantitatively comparing these three diagnostic groups within the same clinically defined cohort. Notably, both gliomas and non-glioma tumors had significantly higher quantitative uptake versus non-tumor lesions, whereas no significant difference was observed between gliomas and non-glioma tumors. Therefore, the principal diagnostic value of ^{18}F-fluciclovine PET in this setting may lie in distinguishing neoplastic from non-neoplastic lesions, rather than specifically identifying the presence of glioma.

^{18}F-fluciclovine is a synthetic amino acid PET tracer whose uptake is mediated by amino acid transport systems, including ASCT2 and LAT transporters [3, 4]. Previous clinical studies have demonstrated high lesion-to-background contrast in gliomas and suggested that ^{18}F-fluciclovine PET had a role in identifying tumor infiltration beyond areas of contrast enhancement on MRI [5-8]. We recently reported an illustrative case wherein ^{18}F-fluciclovine PET detected a small distant glioblastoma lesion that was inconspicuous on conventional MRI, suggesting its utility for detecting biologically active tumor tissue [13]. Thus, ^{18}F-fluciclovine PET may provide complementary information to conventional MRI in the evaluation of glioma.

In the present study, the non-tumor group, which included demyelinating lesions (n = 3) and radiation necrosis (n = 1), had consistently lower ^{18}F-fluciclovine uptake versus both the glioma and non-glioma tumor groups. This distinction is clinically important because contrast-enhancing non-tumor lesions may closely mimic malignant glioma on conventional MRI and create diagnostic uncertainty. The exploratory ROC analysis also showed high AUCs for differentiating glioma from non-tumor lesions, although these estimates should be interpreted cautiously due to the small number of non-tumor cases. Nevertheless, the lower uptake in non-tumor lesions could be attributed to their lower demand for amino acid transport compared to highly cellular tumors. However, ^{18}F-fluciclovine uptake is not specific to tumor tissue; non-tumor lesions may also accumulate the tracer because of activated inflammatory cells, reactive glia, tissue destruction, local perfusion changes, or BBB disruption [14, 15]. Therefore, PET findings should always be interpreted alongside MRI features, longitudinal imaging findings, and the clinical context.

The non-glioma tumor group, consisting predominantly of DLBCL (n = 7) with 2 cases of meningioma, also showed higher uptake than the non-tumor group. This finding emphasizes that ^{18}F-fluciclovine PET uptake is not specific to gliomas. In line with this, substantial amino acid tracer uptake has also been reported in cases of PCNSL [16] and meningiomas [17]. Thus, the potential value of ^{18}F-fluciclovine PET may lie in identifying biologically active neoplastic tissue, rather than in specifically distinguishing glioma from all other tumor types.

Having stronger preoperative support for a tumor diagnosis can be valuable in clinical decision-making regarding the choice between biopsies and resection, selecting sampling targets, and surgical planning that balances maximal tumor control with the preservation of neurological function. In the presence of heterogeneous contrast enhancement, a clearly identifiable ^{18}F-fluciclovine hotspot may help select a sampling target with a higher likelihood of yielding diagnostic tumor tissue. This concept is consistent with the current clinical positioning of amino acid PET as a complementary technique to MRI in the management of glioma [1, 2, 18].

Limitations

This study has several limitations. This was a retrospective, single-center analysis within a relatively small and imbalanced cohort, especially the non-tumor group (n = 4). Since this can influence the estimates of diagnostic performance, including AUCs and the cutoffs selected in this same cohort, these findings should be considered exploratory. Moreover, the sensitivity estimates were based on 13 glioma cases, whereas the specificity estimates were based on only 4 non-tumor cases. Selection bias may have occurred due to the limited availability of PET at our institution, which meant that patients requiring urgent surgery could not undergo preoperative PET. Therefore, our findings may not be generalizable to all patients with suspected malignant glioma. ROI placement was based on contrast-enhancing components, and non-enhancing infiltrative regions were not assessed. The potential effects of scanner settings, reconstruction parameters, and uptake timing on quantitative values were also not fully examined. Lastly, this study did not evaluate the incremental value of ^{18}F-fluciclovine PET over MRI alone, nor its impact on clinical decision-making and outcomes. Larger multicenter studies with external validation are needed to confirm the reproducibility and clinical utility of these quantitative indices.

Conclusion

In this cohort of patients with contrast-enhancing lesions suspected to be malignant glioma, quantitative ^{18}F-fluciclovine PET demonstrated potential for distinguishing neoplastic from non-neoplastic lesions. Quantitative uptake measures and background-corrected metrics showed discriminatory performance, potentially providing valuable adjunctive information for preoperative evaluation. However, since tracer uptake was not specific to glioma, these findings should be interpreted within the broader clinical and radiological context. Further validation in larger prospective cohorts is warranted.

References

1. Law I, Albert NL, Arbizu J, Boellaard R, Drzezga A, Galldiks N, la Fougère C, Langen K-J, Lopci E, Lowe V, McConathy J, Quick HH, Sattler B, Schuster DM, Tonn J-C, Weller M (2019) Joint EANM/EANO/RANO practice guidelines/SNMMI procedure standards for imaging of gliomas using PET with radiolabelled amino acids and [18F] FDG: version 1.0. Eur J Nucl Med Mol Imaging 46:540-557. https://doi.org/10.1007/s00259-018-4207-9

2. Ito K, Jinnouchi S, Kikukawa K, Okuyama C, Sugawara Y, Kawamoto M, Koyama K, Miyake KK, Murakami K (2025) Clinical practice guidelines for 18F-fluciclovine 2024 in the Japanese Society of Nuclear Medicine. Ann Nucl Med 39:899-908. https://doi.org/10.1007/s12149-025-02089-6

3. Okudaira H, Nakanishi T, Oka S, Kobayashi M, Tamagami H, Schuster DM, Goodman MM, Shirakami Y, Tamai I, Kawai K (2013) Kinetic analyses of trans-1-amino-3-[18F] fluorocyclobutanecarboxylic acid transport in Xenopus laevis oocytes expressing human ASCT2 and SNAT2. Nucl Med Biol 40:670-675. https://doi.org/10.1016/j.nucmedbio.2013.03.009

4. Scarpelli ML, Healey DR, Mehta S, Quarles CC (2022) Imaging glioblastoma with 18F-fluciclovine amino acid positron emission tomography. Front Oncol 12:829050. https://doi.org/10.3389/fonc.2022.829050

5. Wakabayashi T, Hirose Y, Miyake K, Arakawa Y, Kagawa N, Nariai T, Narita Y, Nishikawa R, Tsuyuguchi N, Fukami T, Sasaki H, Sasayama T, Kondo A, Iuchi T, Matsuda H, Kubota K, Minamimoto R, Terauchi T, Nakazato Y, Kubomura K, Wada M (2021) Determining the extent of tumor resection at surgical planning with 18F-fluciclovine PET/CT in patients with suspected glioma: multicenter phase III trials. Ann Nucl Med 35:1279-1292. https://doi.org/10.1007/s12149-021-01670-z

6. Parent EE, Benayoun M, Ibeanu I, Olson JJ, Hadjipanayis CG, Brat DJ, Adhikarla V, Nye J, Schuster DM, Goodman MM (2018) [18F] Fluciclovine PET discrimination between high- and low-grade gliomas. EJNMMI Res 8:67. https://doi.org/10.1186/s13550-018-0415-3

7. Michaud L, Beattie BJ, Akhurst T, Dunphy M, Zanzonico P, Finn R, Mauguen A, Schöder H, Weber WA, Lassman AB, Blasberg R (2020) 18F-Fluciclovine (18F-FACBC) PET imaging of recurrent brain tumors. Eur J Nucl Med Mol Imaging 47:1353-1367. https://doi.org/10.1007/s00259-019-04433-1

8. Castello A, Albano D, Muoio B, Castellani M, Panareo S, Rizzo A, Treglia G, Urso L (2023) Diagnostic accuracy of PET with 18F-fluciclovine ([18F] FACBC) in detecting high-grade gliomas: a systematic review and meta-analysis. Diagnostics (Basel) 13:3610. https://doi.org/10.3390/diagnostics13243610

9. Ikemoto T, Hana T, Otsuka N, Murakami C, Kawaguchi Y, Higashi M, Hanakita S (2026) 18F-fluciclovine positron emission tomography uptake is not exclusive to malignant brain tumors: two cases of low-grade and benign lesions with detailed pathological findings. Surg Neurol Int 17:267. https://doi.org/10.25259/SNI_74_2026

10. Sakata A, Takada S, Takeuchi Y, Arakawa Y, Nakamoto Y (2026) 18F-Fluciclovine (18F-FACBC) PET/MRI findings in tumefactive demyelinating lesion: a case report. Clin Nucl Med 51:e779-e781. https://doi.org/10.1097/RLU.0000000000006407

11. World Medical Association (2025) World Medical Association Declaration of Helsinki: ethical principles for medical research involving human participants. JAMA 333:71-74. https://doi.org/10.1001/jama.2024.21972

12. Louis DN, Perry A, Wesseling P, Brat DJ, Cree IA, Figarella-Branger D, Hawkins C, Ng HK, Pfister SM, Reifenberger G, Soffietti R, von Deimling A, Ellison DW (2021) The 2021 WHO classification of tumors of the central nervous system: a summary. Neuro Oncol 23:1231-1251. https://doi.org/10.1093/neuonc/noab106

13. Kagami Y, Hanihara M, Saito R, Kazama H, Yoshioka H (2025) Identification of small distant glioblastoma lesions using 18F-fluciclovine positron emission tomography: illustrative case. J Neurosurg Case Lessons 10: CASE25398. https://doi.org/10.3171/CASE25398

14. Nakajima R, Kimura K, Abe K, Sakai S (2017) 11C-methionine PET/CT findings in benign brain disease. Jpn J Radiol 35:279-288. https://doi.org/10.1007/s11604-017-0638-7

15. Filss CP, Cicone F, Shah NJ, Galldiks N, Langen KJ (2017) Amino acid PET and MR perfusion imaging in brain tumours. Clin Transl Imaging 5:209-223. https://doi.org/10.1007/s40336-017-0225-z

16. Salgues B, Kaphan E, Molines E, Brun G, Guedj E (2021) High 18F-FDOPA PET uptake in primary central nervous system lymphoma. Clin Nucl Med 46:e59-e60. https://doi.org/10.1097/RLU.0000000000003303

17. Arita H, Kinoshita M, Okita Y, Hirayama R, Watabe T, Ishohashi K, Kijima N, Kagawa N, Fujimoto Y, Kishima H, Shimosegawa E, Hatazawa J, Hashimoto N, Yoshimine T (2012) Clinical characteristics of meningiomas assessed by 11C-methionine and 18F-fluorodeoxyglucose positron-emission tomography. J Neurooncol 107:379-386. https://doi.org/10.1007/s11060-011-0759-2

18. Galldiks N, Lohmann P, Fink GR, Langen KJ (2023) Amino acid PET in neurooncology. J Nucl Med 64:693-700. https://doi.org/10.2967/jnumed.122.264859

Statements and Declarations

Funding

No specific funding was received for this study.

Competing Interests

The authors have no relevant financial or non-financial interests to disclose.

Author Contributions

Ryu Saito contributed to the study conception and design, data collection, image analysis, statistical analysis, and manuscript drafting. Mitsuto Hanihara contributed to the study conception and design, supervised the study, and critically revised the manuscript. Hirofumi Kazama contributed to data collection, image analysis, and manuscript revision. Hideyuki Yoshioka supervised the research and critically revised the manuscript. All authors read and approved the final manuscript.

Data Availability

The data supporting the findings of this study are available from the corresponding author upon reasonable request.

Ethics Approval

This study was performed in accordance with the principles of the Declaration of Helsinki. The study protocol was approved by the University of Yamanashi Ethics Committee (approval no. 2845).

Consent to Participate

The requirement for individual informed consent was waived by the University of Yamanashi Ethics Committee (approval no. 2845). Information about the study was publicly disclosed, and patients were provided with the opportunity to decline the use of their clinical data through an opt-out procedure.

Consent to Publish

Not applicable. All clinical imaging and histopathological images included in this manuscript have been anonymized and contain no patient-identifying information.

Figure legends

Fig. 1 Quantitative comparison of ^{18}F-fluciclovine PET uptake parameters among glioma, non-glioma tumor, and non-tumor lesions
Box-and-whisker plots with individual data points illustrate SUVmax, SUVpeak, T/B ratio, Tpeak/B ratio, and background white matter SUVmean (SUVmean_B) across the three diagnostic groups. Center line, median; box, interquartile range; whiskers, data points within 1.5 times the interquartile range. Post hoc Dunn's test with Holm correction demonstrated significantly higher SUVmax, SUVpeak, T/B ratio, and Tpeak/B ratio in both the glioma and non-glioma tumor groups versus the non-tumor group. SUVmean_B did not differ significantly across the three groups. *$P < 0.05$

Fig. 2 Diagnostic performance of the quantitative ^{18}F-fluciclovine PET parameters for differentiating glioma from non-tumor lesions
Receiver operating characteristic curves comparing glioma (n = 13) versus non-tumor lesions (n = 4) in terms of SUVmax, SUVpeak, T/B ratio, and Tpeak/B ratio. AUCs were 0.981 (95% CI, 0.885–1.000), 0.981 (95% CI, 0.885–1.000), 0.962 (95% CI, 0.846–1.000), and 0.962 (95% CI, 0.846–1.000), respectively. Youden-derived cutoffs were 3.190, 2.520, 10.633, and 8.400, respectively, with a sensitivity of 92.3% (12/13) and specificity of 100% (4/4) at each cutoff. The cutoffs and their apparent performance are considered exploratory.

Fig. 3 Case 2: MRI, ^{18}F-fluciclovine PET, and pathological findings
Axial FLAIR sequence revealing a lesion in the left frontal lobe associated with surrounding edema (a). Contrast-enhanced T1WI demonstrating an irregular ring-like pattern of enhancement around the lesion (b). Coregistered ^{18}F-fluciclovine PET and contrast-enhanced T1WI demonstrating an overlap of radiotracer accumulation with the enhancing lesion, with an SUVmax of 8.20 and SUVpeak of 6.45 (c). Hematoxylin and eosin staining showing diffuse proliferation of atypical glial cells with microvascular proliferation, confirming the diagnosis of glioblastoma (original magnification, ×200) (d)

Fig. 4 Case 25: MRI, ^{18}F-fluciclovine PET, and histopathological findings
Axial FLAIR imaging depicting a right frontal lobe lesion with perilesional edema (a). Contrast-enhanced T1WI demonstrating irregular ring-like enhancement (b). Fusion of ^{18}F-fluciclovine PET with contrast-enhanced T1WI confirming concordance between tracer uptake and the area of enhancement, with an SUVmax of 1.38 and SUVpeak of 1.00 (c). Hematoxylin and eosin staining showing marked infiltration of foamy macrophages and perivascular inflammatory cells, without atypia or proliferation of glial cells, supporting the diagnosis of demyelinating disease (original magnification, ×200) (d)